IEEE Access
Multidisciplinary | Rapid Review | Open Access Journal

Received 20 October 2022, accepted 9 November 2022, date of publication 14 November 2022, date of current version 18 November 2022.

Digital Object Identifier 10.1109/ACCESS.2022.3221813

RESEARCH ARTICLE

Gait-Based Continuous Authentication Using a Novel Sensor Compensation Algorithm and Geometric Features Extracted From Wearable Sensors

SOOBIN LEE[1], SEUNGJAE LEE[1], EUNKYOUNG PARK[2], JONGSHILL LEE[1], AND IN YOUNG KIM[1]

[1]Department of Biomedical Engineering, Hanyang University, Seoul 04763, South Korea
[2]Department of Medical and Mechatronics Engineering, Soonchunhyang University, Asan 31538, South Korea

Corresponding authors: Jongshill Lee (netlee@hanyang.ac.kr) and In Young Kim (iykim@hanyang.ac.kr)

This work was supported in part by the Institute of Information and Communications Technology Planning and Evaluation (IITP) Grant through the Korean Government [Ministry of Science and ICT (MSIT)], Development of Connected Medical Device Anti-Hacking Technology for Safe Medical/Healthcare Services (50%), under Grant 2020-0-00447; and in part by the Basic Science Research Program through the National Research Foundation of Korea (NRF) funded by the Ministry of Education, Development of Biometric Authentication Technology Based on Gait Using Smart Devices (50%), under Grant 2021R1I1A1A01055813.

This work involved human subjects or animals in its research. Approval of all ethical and experimental procedures and protocols was granted by the Institutional Review Board (IRB) of Hanyang University under Approval No. HYUIRB-202112-008.

ABSTRACT With the rapid development of networking and computing technology, users can easily store and interact with sensitive information on smart devices. Since smart devices are vulnerable to unauthorized access or theft, the security of personal information is becoming more important. Gait authentication is attracting attention as a continuous or unconscious biometrics method for smart devices. However, various factors, such as gait variability and sensor state by day, can degrade authentication performance. This study proposed a sensor compensation algorithm that overcomes various factors that may occur in the real world and new 2D cyclogram features to improve user authentication performance. The dataset consists of gait data from 20 people wearing wearable sensors on the wrist and thigh over 3 days. A support vector machine (SVM) model was used for the classification of gait authentication. The results showed that the proposed sensor compensation algorithm could obtain a consistent gait signal by transforming the unstable sensor coordinate system into a stable anatomical coordinate system. Also, 2D cyclogram feature sets could be used to effectively discriminate individual gait patterns. The proposed gait authentication has an accuracy of 99.63%, 94.16%, and 94.2% and an equal error rate (EER) of 0.3%, 5.84%, and 5.8% for the same session (day 1), cross session1 (day 2), and cross session2 (day 3), respectively.

INDEX TERMS Authentication, biometrics, gait recognition, wearable sensor, machine learning.

I. INTRODUCTION

The computing and networking technologies of smart devices have been rapidly developing, and they help users to process complex online tasks (e.g., mobile banking, business, social network service, and healthcare). Smart devices have become an essential part of our daily life and are used to access and store sensitive/confidential information. Indeed, the data stored within smart devices are likely to be of much greater value than the device itself [1]. With the pervasiveness of these devices, security is becoming more crucial. Currently, authentication processes used to protect personal information are conventionally grouped into knowledge-based, token-based, and biometrics-based categories [2]. Knowledge-based authentication methods (e.g., password, pin, and pattern) represent a process in which a user must remember

The associate editor coordinating the review of this manuscript and approving it for publication was Vincenzo Conti.

a string of data. However, this method relies on memory, causing possible user inconvenience. Also, this approach is vulnerable to smudge attacks [3], which use fingerprint smudges on the touch screen to extract sensitive information, and shoulder surfing attacks [4] caused by deliberate spying. Token-based authentication methods (e.g., bank smartcard, OTP, and short messaging service) use a physical key in the possession of a user. However, this method has the disadvantage of risk of loss and leak [5].

Finally, biometrics-based authentication methods utilize unique human characteristic information. Biometrics are divided into physiological and behavioral characteristics. Physiological characteristics include the face, fingerprint, and iris which are signals measured directly from the semi-permanent part of the body, and behavioral characteristics include gait, voice, and signature that can be indirectly measured during specific behaviors [6]. Since biometric identifiers are inherently individual, it is more difficult to manipulate, share, or forget these traits [7]. Hence, biometric traits are widely used as an efficient method to protect personal information.

However, existing methods of physiological biometrics are vulnerable to user spoofing attacks. For example, fingerprints can be duplicated using clay or 3D-printing technology [8], [9] and the face and iris can be replicated using 2D image capture [10], [11], [12]. To overcome these limitations, we are focusing on the use of behavioral biometrics, as they are more difficult to imitate than physiological biometrics [13].

Behavioral biometrics using human gait (walking style) have many advantages over other behavioral biometrics. Many studies, including in the fields of psychology, medicine, and biometrics, suggest that human gait has unique individual characteristics [14], [15] that can be used as identifiers to distinguish individuals [16]. In addition, gait imitation requires a lot of effort and concentration, so it is strong against spoofing attacks [17]. Gait data can be readily acquired from the sensors embedded in smart devices without additional equipment. Such data can be applied for continuous and unconscious verification of user identity without direct interaction.

Despite the above advantages, the available sensor-based gait authentication methods have limitations. First, the permanence of such algorithms has not been verified. Most studies evaluate the performance of algorithms through the same-session scenario [18], [19], [20]. Such scenarios cannot account for variability in user gait patterns, as enrollment and test data are collected on the same day/session. Therefore, we need to validate the performance of the algorithm in a cross session scenario that utilizes data collected from multiple days/sessions.

Second, existing gait authentication studies do not consider the instability of the sensor coordinate system, which is easily affected by the sensor's placement, orientation, and dynamic behavior. An unstable coordinate system causes inconsistent signals despite the same behavior pattern. In particular, when measuring over several days, it is likely to acquire irregular

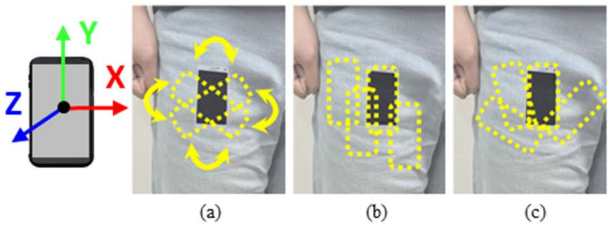

FIGURE 1. Mobile coordinate system and axis error caused by sensor statement and movement. (a) Disorientation error, (b) Misplacement error, (c) Disorientation error and misplacement error.

data due to changes in sensor wearing state on the user body. An unstable coordinate system can lead to incorrect gait analysis and poor authentication performance. Therefore, it is necessary to address various errors (Fig. 1) occurring in daily life into a stable coordinate system by compensating in real-time.

Based on the above brief background, we propose a novel gait authentication method based on wearable sensors.

The main contributions of this paper are as follows.

1) We constructed a dataset that considers gait variability over time and various sensor coordinate systems that can be experienced in real-life.
2) We propose a sensor compensation algorithm that transforms an unstable sensor coordinate system into a stable anatomical coordinate system in real-time.
3) We describe a novel feature extraction method that can extract robust and discriminative features from gait signals.
4) Finally, we analyze the effects of sensor position and number of gait cycles on authentication performance.

The rest of this paper is organized as follows. Section II introduces related works in gait authentication. Section III explains the proposed authentication framework in detail. Section IV describes the experimental results to evaluate the proposed framework. Section V consists of a discussion of the proposed framework. Section VI presents the conclusion and future works.

II. RELATED WORKS

A. CONTINUOUS USER AUTHENTICATION

Continuous user authentication is an unconscious process of verifying a user based on behavioral attributes [21], also called ''transparent,'' ''implicit,'' ''non-intrusive,'' ''non-observable,'' or ''unobtrusive'' [22]. Gait corresponds to continuous authentication, and it is divided into vision-based, floor sensor-based, and wearable sensor-based according to the data collection method. Vision-based methods use a camera to recognize gait patterns in images and analyze their characteristics [23], [24]. Floor sensor-based methods utilize a pressure sensor on the floor to analyze ground reaction force (GRF) or heel-to-toe ratio [25], [26], [27]. The wearable sensor-based method analyzes various signals (e.g., accelerometer, gyroscope, and angle) collected by a sensor attached to the body. Recently, most gait authentication

studies have focused on wearable sensor methods that can be easily deployed and directly represent the dynamics of gait. This method has emerged as the most promising method for user authentication based on gait.

B. WEARABLE SENSOR-BASED GAIT AUTHENTICATION

Cola et al. proposed a gait authentication method that relies on an acceleration signal acquired at the user's wrist [18]. The experiments were carried out under controlled conditions by 15 volunteers. The researchers segmented gait cycles based on the dominant peak and removed irregular gait cycles using an autocorrelation coefficient. Fifteen to nineteen features that express individual gait characteristics were extracted per cycle. Regarding authentication, the method utilized semi-supervised anomaly detection, which uses Euclidean distance and Nearest Neighbor Analysis to determine the anomaly score. The result obtained an Equal Error Rate (EER) of about 4.5%.

Xu et al. presented devices and algorithms that enable gait authentication in a low-power state [28]. In that study, gait data were acquired through the developed device held in the hand during a 5-minute walk during 2 sessions performed by 20 people. The method used Single Value Decomposition (SVD) to eliminate noise. The authentication model is trained through dictionary learning and tests new data according to the learned probabilities. The proposed system achieved an average EER of 12.65%.

Johnston et al. proposed an authentication method using acceleration and gyroscope data measured by a commercial smartwatch [19]. The researchers recorded 5-minute gait data from 59 volunteers. The obtained signal is divided into sliding windows, and 43 features are extracted for each window. They used Naïve Bayes (NB), Random Forest (RF), and Multi-Layer Perceptron (MLP) classifiers and achieved average EERs of 2.6% and 8.1%, respectively, for each user signal (acceleration, gyroscope).

Alobaidi et al. investigated the possibility of authenticating users performing multiple actions over multiple days [29]. To do so, data were acquired from accelerometer and gyroscope sensors in commercial smartphones (in a belt pouch). The data were recorded over an average of 8 days for 44 people, and 304 features were extracted in the time and frequency domains. The model uses an MLP to classify behavior and authenticate users and achieved an EER of 11.38%, 11.32%, 24.52%, and 27.33% for normal walking, fast walking, and walking down and up stairs, respectively.

Hoang et al. addressed sensor orientation instability in gait signal validation [20]. Thirty-eight volunteers collected acceleration, orientation, and gravity data on gait for 10 minutes while wearing a smartphone in a trouser pocket. Only one axis was fixed based on the direction of gravity acceleration. Twenty-nine features extracted in the time and frequency domains were selected by Principal Component Analysis (PCA). User authentication performance with Support Vector Machine (SVM) showed a 2.4% EER.

C. LIMITATIONS OF EXISTING WORKS

In order to use gait data for safe and convenient biometrics, the following characteristics must be ensured [30].

1) Permanence: traits should not change over time
2) Distinctiveness: traits should be helpful in distinction between people
3) Performance: traits should be highly efficient

However, it is difficult to confirm the permanence of authentication algorithms because previous gait data were acquired for only 1 day/session [18], [19], [20]. Previous studies did not consider complex problems caused by the instability of the coordinate system [18], [19], [28], [29]. Another study implemented a compensation algorithm but could not easily determine conversion into a stable coordinate system because only one of the three axes of acceleration measured by the sensor is fixed [20]. Finally, most existing works only extract statistical features, missing the distinct behavioral attributes among individuals.

To address the above challenges, we constructed a multi-day gait dataset and proposed a real-time coordinate compensation method based on pedestrians and a novel feature extraction method based on a cyclogram.

III. METHODS

A. METHODOLOGY OVERVIEW

As shown in Figure 2, the workflow of our framework mainly consists of three steps: 1) data collection, 2) data processing, and 3) user authentication. In the data collection step, the subjects wear a device embedding a 9-axis IMU sensor on their right thigh and left wrist. Gait data composed of acceleration and Euler angle are collected over 3 sessions. User authentication is achieved using 3-axis acceleration, and the 3-axis Euler angle is used during data processing. The data processing step comprises noise removal and gait cycle segmentation. The segmented gait cycle is compensated based on a stable anatomical plane to mitigate disorientation and misplacement errors caused by unstable sensor coordinate systems. User authentication step, individual feature sets are extracted not only 1D statistical features but also 2D cyclogram features including distinct behavioral attributes. Then, based on the selected individual optimized feature set, user authentication is performed through machine learning method. All stages of the proposed framework are explained in detail in the following sections.

B. DATA COLLECTION

We developed a gait measurement system (GMS) to measure and analyze gait data. The system includes a microcontroller (STM34F411CEU, STMicroelectronics, Switzerland), a Bluetooth module (PAN1321i, Panasonic, Japan), and a 9-axis inertial measurement unit (BNO055, BOSCH, Germany), as shown in Fig. 3(a). Gait data were measured at two positions (right thigh and left wrist), based on a common placement of smart devices (i.e., smart phone and smart watch), as shown in Fig. 3(b) and (c).

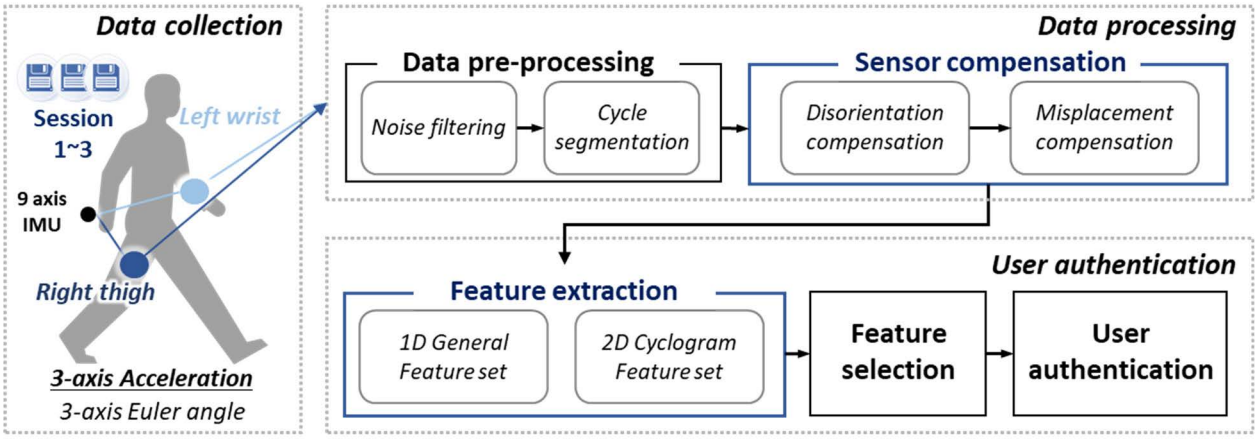

FIGURE 2. System overview of the proposed method for user authentication.

The developed GMS measures gait data, including acceleration and Euler angle, at a sampling rate of 100Hz. Acceleration is measured in meters per second squared (m/s^2) in the X, Y, and Z axes. The Euler angle is calculated through BOSCH's sensor fusion algorithm [31] and is represented as the rotation angle (°) of the GMS based on Heading (yaw), Roll, and Pitch axes. The Euler angle is used to detect gait events [32], [33] and detect gravity for sensor calibration. In this study, the acceleration signal is the focus on analysis, and the Euler angle is utilized to assist the acceleration signal processing.

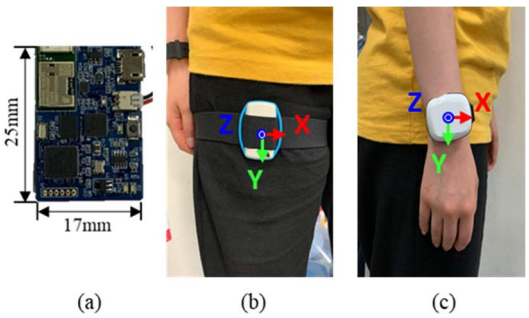

FIGURE 3. Gait measurement system (GMS) and its positions of (a) the sensor module of the GMS (b) at the thigh and (c) at the wrist.

The study recruited 20 subjects (13 males and 7 females) aged between 23-31 years. All subjects participated in 3 data collection sessions within 7 days. Among the 3 sessions, the data are referred to as same session for the first day, and data from the second and third test days are called Cross session 1 and Cross session 2, respectively. Subjects wore the GMS freely and walked a 50 m hallway at normal gait speed, which is defined as in 1 phase. In order to induce various sensor axis errors as experienced in the real world, the subjects wore the GMS again freely for 4 phases. The gait data consist of 1600 m (50 m × 32phase) in the same session, 1200m (50 m × 24 phases) in cross session 1, and 1200m (50m × 24 phases) in cross session 2. Thus,

TABLE 1. Detail information of gait dataset.

Property	Value
Subject	20 (13 males, 7 females)
Age	23~30
Height	154~188 cm
Weight	47~ 95 kg
Measurement position	Right thigh & Left wrist
Recording session	3 sessions within 7 days
Environment	50 m indoor hallway
Walking distance	Same session : 1,600 m (Day1) Cross session1,2 : 1,200 m (Day2 & Day3)
Sensor state	Disorientation : −60°~60° based on frontal plane Misplacement : 0 ~90° lateral rotation based on transverse plane Rotation sensor each 200 m (4phase)

we can represent the sensor state of putting the device in a trouser pocket or wearing a watch. More details of the data collection are summarized in Table 1. The IRB of Hanyang University approved this study, and all subjects supplied informed consent before the experiment (HYUIRB-202112-008).

C. DATA PREPROCESSING

1) NOISE FILTERING

The measured acceleration signal comprises various components, as described in Equation (1):

$$ACC_{sensor} = ACC_{movement} + ACC_{noise} + ACC_{gravity} \quad (1)$$

In order to analyze only $ACC_{movement}$, it is necessary to remove ACC_{noise} and $ACC_{gravity}$.

Considering the typical stride frequency of a healthy person and the Nyquist theorem, the cut-off frequency should be higher than 2.5 Hz [34]. In the present study, ACC_{noise} was removed using the fifth Butterworth low pass filter and a 2.5 Hz cut-off frequency. The $ACC_{gravity}$ removal method is described in Section D.

TABLE 2. Remain ratio of gait cycles according to PCC value threshold.

PCC Value	0.7	0.75	0.8	0.85	**0.9**	0.95
Thigh	99.39	99.39	99.36	99.33	**99.19**	98.76
Wrist	98.56	98.20	97.57	96.62	**94.60**	88.84

2) CYCLE SEGMENTATION & OUTLIER CYCLE REMOVAL

In analysis, the gait signal consists of a periodic segment called a gait cycle, each of which starts and ends with a heel strike [20]. In this section, we describe a method of segmenting and removing the gait cycle. When performing gait cycle segmentation, it is necessary to determine heel strike and gait length. Heel strike is detected based on the Euler angle [32], which is reflected in the acceleration signal and is set as the start point (sp) of a gait cycle. A previously defined cycle segmentation method [13] is performed to estimate the cycle length. First, the segmentation method estimates the length (L_e) of the gait cycle using a Fast Fourier Transform (FFT). Then, the starting point of the acceleration signal (sp) and estimated length (L_e) are used to accurately obtain the gait length (d), as shown in Equations (2) and (3).

$$sp_N + L_e - d < sp_{N+1} < sp_N + L_e + d \tag{2}$$

$$d = 0.3 \times L_e \tag{3}$$

Next, we eliminate outlier cycles caused by stumbling and other factors. All subjects performed an average of 30 cycles during 1 phase. To remove the outlier cycles, we calculate the Pearson Correlation Coefficient (PCC) [35] between each cycle and the reference average cycle. The PCC value ranges between $+1$ and -1, and any calculated PCC value beyond the set threshold is removed as an outlier. We select an appropriate outlier filtering threshold with a threshold of 0.7 to 0.95. As shown in Table 2, the remain ratio of gait cycles is similar between threshold 0.7 and 0.9, but many cycles are rapidly removed at threshold 0.95. We set the outlier filtering threshold to 0.9, taking into account the remain ratio of gait cycles and the degree of freedom of the measurement position. Fig.4 presents the 3-axis acceleration cycle before and after the outlier cycle removal process.

D. SENSOR COMPENSATION

An important complication of authentication based on gait signals is to solve an unstable sensor coordinate system. The instability of the coordinate system affects the quality of the acquired gait signals, leading to inaccurate analysis and lower authentication performance. Therefore, the unstable sensor coordinate system (X, Y, Z) must be transformed into a stable pedestrian anatomical plane (Medial-Lateral, Superior-Inferior, Anterior- Posterior [36]). In this section, we explain compensation methods for disorientation and misplacement errors mentioned in Section A.

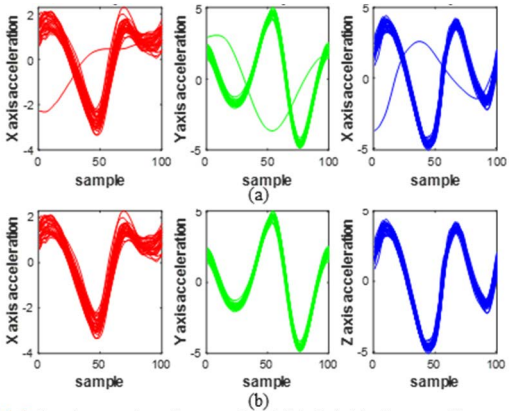

FIGURE 4. 3 axis acceleration cycle at thigh (a) before outlier cycle removal (b) after outlier cycle removal.

1) DISORIENTATION COMPENSATION

To compensate for disorientation error, we utilize gravity, the Earth-fixed coordinate, as a reference. First, we compute the 3-axis gravity acceleration component based on the extracted Euler angle [37], [38]. Next, we calculate a rotation matrix R^T that transforms the Y axis of the sensor coordinate system to be parallel to the direction of gravity acceleration as in Equations (4)-(8)

$$\boldsymbol{A}^{(X,Y,Z)} = (\boldsymbol{a}^{(X)}, \boldsymbol{a}^{(Y)}, \boldsymbol{a}^{(Z)}) \tag{4}$$

where A is the 3-axis acceleration values measured by the GMS,

$$\boldsymbol{G}^{(X,Y,Z)} = (\boldsymbol{g}^{(X)}, \boldsymbol{g}^{(Y)}, \boldsymbol{g}^{(Z)}) \tag{5}$$

where G represents the 3-axis gravity acceleration values calculated based on the mentioned reference. All gravity acceleration components are aligned along the Y axis to transform into a fixed-coordinate system.

$$\theta_i^{(X)} = \text{acos}\left(\frac{abs\left(\boldsymbol{g}_i^{(Y)}\right)}{\sqrt{\left(\boldsymbol{g}_i^{(Y)}\right)^2 + \left(\boldsymbol{g}_i^{(Z)}\right)^2}}\right) \tag{6}$$

$$\theta_i^{(Z)} = \text{acos}\left(\frac{abs\left(\boldsymbol{g}_i^{(Y)}\right)}{\sqrt{\left(\boldsymbol{g}_i^{(Y)}\right)^2 + \left(\boldsymbol{g}_i^{(X)}\right)^2}}\right) \tag{7}$$

where $\theta_i^{(X)}$ and $\theta_i^{(Z)}$ are the angles between the gravity components aligned with the Y axis ($\boldsymbol{G[0,1,0]}$) and $\boldsymbol{a}^{(X)}, \boldsymbol{a}^{(Z)}$.

$$\begin{aligned} R_i^{(T)} &= {}_i^{(X)} \times R_i^{(Z)} \\ &= \begin{bmatrix} 1 & 0 & 0 \\ 0 & cos\theta_i^{(X)} & -sin\theta_i^{(X)} \\ 0 & sin\theta_i^{(X)} & cos\theta_i^{(X)} \end{bmatrix} \\ &\quad \times \begin{bmatrix} cos\theta_i^{(Z)} & sin\theta_i^{(Z)} & 0 \\ -sin\theta_i^{(Z)} & cos\theta_i^{(Z)} & 0 \\ 0 & 0 & 1 \end{bmatrix} \end{aligned} \tag{8}$$

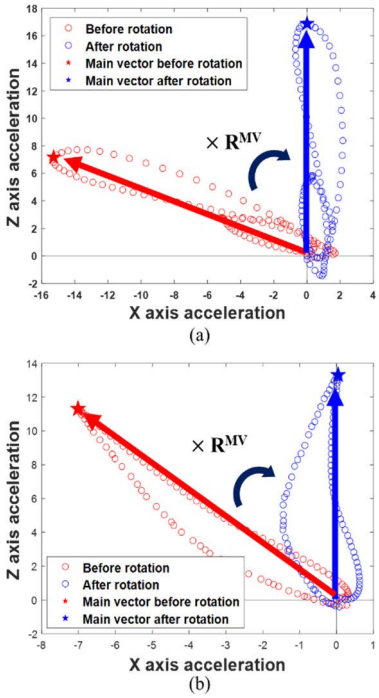

FIGURE 5. Example of the main vector rotation before and after (a) at the thigh and (b) at the wrist.

The influence of the gravity component is removed to obtain the $ACC_{movement}$ signal, as in Equations (9) and (10).

$$\boldsymbol{A}_i^{(X,SI,Z)} \leftarrow \boldsymbol{A}_i^{(X,Y,Z)} \times R_i^{(T)} \tag{9}$$

$$\boldsymbol{A}_i^{(SI)} \leftarrow \boldsymbol{A}_i^{(SI)} - \boldsymbol{G}_i^{(Y)} \tag{10}$$

The acceleration signals after disorientation compensation are not affected by gravity, and the Y axis is parallel to gravity. In other words, the Y axis is transformed into the SI axis of the proposed fixed-coordinate system.

2) MISPLACEMENT COMPENSATION

To compensate for misplacement error, we utilize a main vector that represents the actual walking direction. The main vectors of the X and Z axes ($\boldsymbol{A}_i^{(X_{MV})}$ and $\boldsymbol{A}_i^{(Z_{MV})}$) for each stride are set as the maximum value of the Root Mean Square (RMS) of both accelerations. The angle ($\theta_i^{(MV)}$) and rotation matrix ($R_i^{(MV)}$) for the main vector are calculated as described in Equations (11) and (12).

$$\theta_i^{(MV)} = \text{acos}\left(\frac{abs\left(\boldsymbol{A}_i^{(Z_{MV})}\right)}{\sqrt{\left(\boldsymbol{A}_i^{(X_{MV})}\right)^2 + \left(\boldsymbol{A}_i^{(Z_{MV})}\right)^2}}\right) \tag{11}$$

$$R_i^{(MV)} = \begin{bmatrix} cos\theta_i^{(MV)} & sin\theta_i^{(MV)} & 0 \\ -sin\theta_i^{(MV)} & cos\theta_i^{(MV)} & 0 \\ 0 & 0 & 1 \end{bmatrix} \tag{12}$$

As shown in Fig. 5, the main vector is transformed to the AP axis through the rotation matrix ($R^{(MV)}$). Finally, we obtain a stable coordinate system by fixing the two-axis coordinate system.

$$\boldsymbol{A}_i^{(ML,SI,AP)} \leftarrow \boldsymbol{A}_i^{(X,SI,Z)} \times R_i^{(MV)} \tag{13}$$

In addition, by transforming the X, Y, and Z axes of the sensor to the Medial-Lateral (ML), Superior-Inferior (SI), and Anterior-Posterior (AP) axes of the anatomical plane, respectively, as in Equation (13), we can analyze the gait based on the user rather than that of the sensor.

TABLE 3. List of 1D general features for user authentication.

Feature	Position	Axis	Description
Max	Both [a]	All [b]	The largest value in a cycle
Min	Both	All	The smallest value in a cycle
Mean	Both	All	The mean value in a cycle
Median	Both	All	The median value in a cycle
RMS	Both	All	The square root of the mean squared
Max to Min	Both	All	The difference between max and min values
Variance	Both	All	The variance in a cycle
Correlation	Both	All	The relationship between the two axes
Kurtosis	Both	All	A measure of the shape of the curve
Skewness	Both	All	A measure of the symmetry of the data
IQR	Both	All	The median of the lower and upper halves of the cycle data
Peak slope	Both	SI	The slope between the two peaks
Acceleration at 50	Both	SI	Acceleration value at 50 sample

[a]Both refers to use of measured signals from the thigh and wrist. [b]All refers to extraction of features from three axes (ML, SI, and AP); RMS = Root Mean Square, IQR = Interquartile Range.

E. FEATURE EXTRACTION

Previous studies mainly used statistical features for gait authentication (e.g., min, max, mean, median, etc.) [18], [19], [20], [29]. However, it is difficult to reflect the distinctiveness and permanence of gait characteristics with only statistical features, which may lead to deterioration of authentication performance. Therefore, we additionally consider the behavioral and mechanical features that can represent the characteristics of an individual's gait.

In this study, we utilize two kinds of feature sets to reflect various gait components. First, the "general feature set" extracts statistical and non-statistical features based on previous research. As shown in Table 3, the general feature set consists of 70 features (35 thigh features and 35 wrist features).

Next, to extract robust and distinct features, we propose a "cyclogram feature set" comprised of gait events and cyclogram morphology. The cyclogram represents a two-dimensional geometric pattern using two one-dimensional time-series signals and is conventionally used to diagnose gait diseases through the relationship of the Euler angles between two segments [39]. This has the advantage of extracting morphological features that cannot be represented

TABLE 4. List of 2D cyclogram feature sets for user authentication.

Analysis category	Features	Position	Plane	Description
Gait event	ACC of HS	Both	ALL	Acceleration at heel strike
	ACC of TO	Both	ALL	Acceleration at toe-off
	Stance phase	Both	AP	Time the foot is on the ground (sample)
	Swing phase	Both	AP	Time the foot is in the air (sample)
	Phase ratio	Both	AP	Ratio of the swing phase to the stance phase
	Walking speed	Both	AP	Time per stride before normalization (sample)
Curvature	Curvature	Both	ALL	Curvature of the whole cyclogram
	Curvature in ST	Both	ML	Curvature of the cyclogram in the stance phase
	Curvature in SW	Both	ML	Curvature of the cyclogram in the swing phase
Length & Slope	Cyclogram length	Both	ALL	Sum of the lengths between vectors
	SW cyclogram length	Both	ALL	Sum of the lengths between vectors in the stance phase
	ST cyclogram length	Both	ALL	Sum of the lengths between vectors in the swing phase
	CM length	Both	ALL	Length between the center of mass and origin (0,0)
	CM length in ST	Both	ALL	Length between the center of mass and origin (0,0) in the stance phase
	CM length in SW	Both	ALL	Length between the center of mass and origin (0,0) in the swing phase
	Max to Min length	Only thigh	ML	Length between the max point based on AP and min point based on SI (a)
	Max to Min in ST length	Only thigh	SI	Length of the max point to the min point based on the AP axis in the stance phase (b)
	Max to Min in ST slope	Only thigh	SI	Slope of the max point to the min point based on the AP axis in the stance phase (b')
	Max to Min in SW length	Only thigh	SI	Length of the max point to the min point based on the AP axis in the swing phase
	Max to Min in SW slope	Only thigh	SI	Slope of the max point to the min point based on the AP axis in the swing phase
	CMSW to CMST slope	Only wrist	SI	Slope of the center of mass in the swing phase to the center of mass in the stance phase (c)
	Left- & right-side peak slope	Only wrist	ML	Slope of the maximum points based on the SI axis in the swing and stance phases (d)
Area	3 CM area	Both	ALL	Area of three centers of mass (total, stance, and swing phases)
	ST area	Only thigh	ML	Area of the stance phase
	SW area	Only thigh	ML	Area of the swing phase
	e area	Only thigh	ML	Area of the negative range based on the AP axis of the stance phase (e)
	f area	Only wrist	SI	Area of the whole cyclogram
	Left-side area	Only wrist	ML	Area of the left cyclogram of intersection(g)
	Right-side area	Only wrist	ML	Area of the right cyclogram of intersection(g')
Angle	h angle	Only thigh	AP	Angle between the SI max points in the swing phase & stance phase

HS = Heel Strike, TO = Toe-off, ST = Stance phase, SW = Swing phase, CM = Center of Mass, CMSW = Center of Mass in Swing phase, CMST = Center of Mass in Stance phase

with 1D signals using gait events and mechanical characteristics within the gait cycles. Therefore, we propose a new feature extraction method that applies acceleration signals to a cyclogram. As shown in Fig. 6, the cyclograms show different aspects depending on the acceleration of each axis. Acceleration data for each axis include unique patterns and characteristics of each person due to walking style, walking speed, and physical differences. Table 4 describes the extracted cyclogram features of gait event, curvature, length, slope, area, and angle for each plane. The cyclogram feature set consists of 88 features (46 thigh features and 42 wrist features), each of which is extracted differently depending on measurement position and axis/plane.

F. FEATURE SELECTION

To obtain individual optimized feature sets and improve the personal authentication performance, we applied a feature selection method called the Relif-F algorithm [40]. The input data uses only a training portion of the same session data. The output of Relif-F is a weight with a range of -1 to 1, and the more important prediction feature, the larger the weight. $X = \{x_1, x_2, \ldots, x_{81}\}$ and $Y = \{y_1, y_2, \ldots, y_{77}\}$ are feature vectors extracted from the thigh and wrist, respectively. The selected feature vectors X' and Y' consist only of features with positive weights in X and Y. It is selected differently for each person according to their walking characteristics, and the number of features is $65 \sim 86$ in the thigh(X') and $42 \sim 78$ in the wrist(Y').

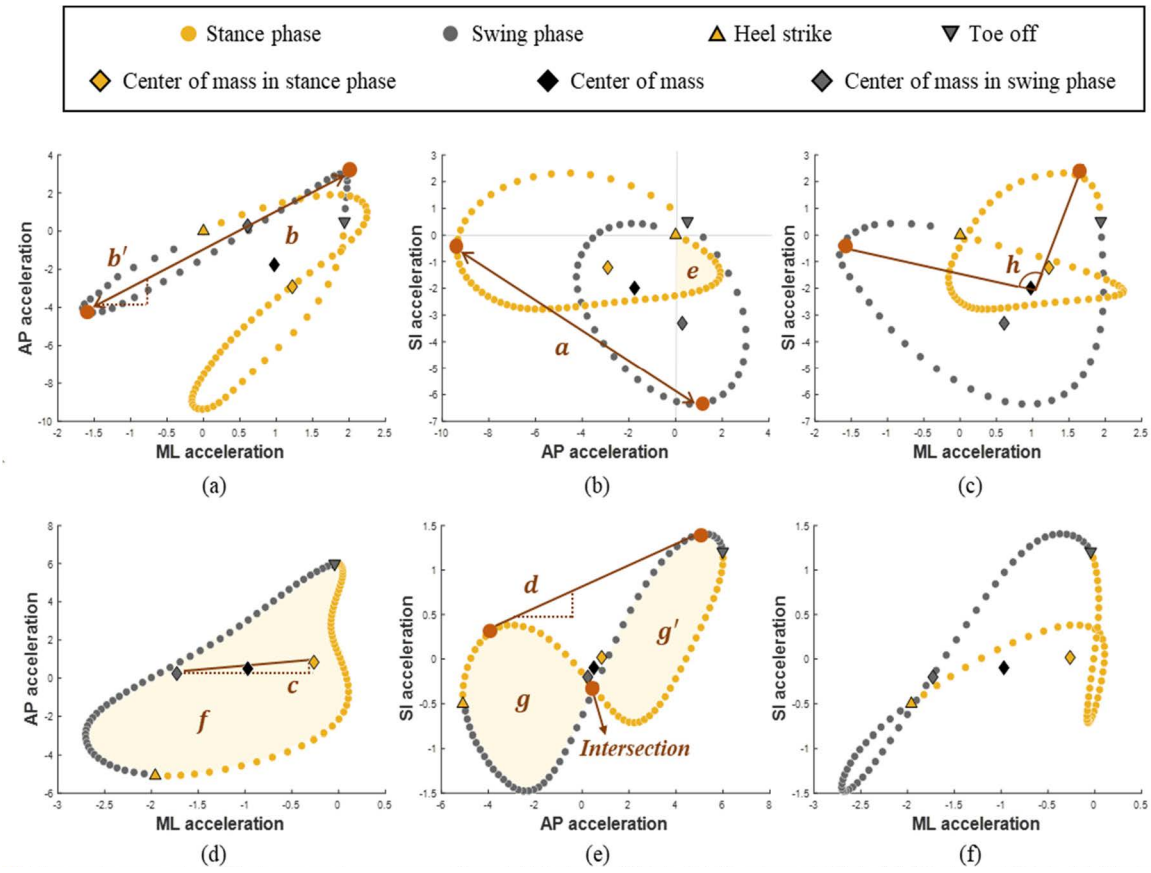

FIGURE 6. The cyclogram of all 2D planes and sensor positions (a) SI plane at thigh, (b) ML plane at thigh, (c) AP plane at thigh, (d) SI plane at wrist, (e) ML plane at wrist, (f) AP plane at wrist.

G. USER AUTHENTICATION

1) DATA DESCRIPTION

Gait cycle data were collected from 20 participants in 3 sessions using GMS according to the experimental protocol. The collected gait dataset consists of 20,122 cycles in the same session, 14,724 cycles in cross session 1, and 14,949 cycles in cross session 2. The average number of cycles per person is 1006 cycles, 736 cycles, and 747 cycles in the respective sessions. Finally, user authentication is performed with a personal optimization feature set extracted from each cycle. We generate individual authentication models by extracting only the selected feature vectors for each cycle. Finally, user authentication is performed with an optimization model per person.

2) AUTHENTICATION

We created an individual authentication model using a linear SVM with 10-fold cross-validation as a classifier. The order of authentication performance evaluation is constructed considering the actual biometrics enrollment sequence. First, we randomly selected the same session data for each subject and split it at a 70:30 ratio. The training set contained 70% of the same session data, and the test set contained the remaining 30% of the same session data and both cross session 1 and cross session 2 data.

IV. RESULTS

In this section, we evaluate the performance of the proposed authentication method. First, the sensor compensation algorithm is validated using the similarity analysis between the compensated and non-compensated gait data. Second, we compare the authentication performance between the general feature set extracted from 1D acceleration data and the 2D cyclogram feature set. Finally, the effects of sensors in different positions and the number of gait cycles on performance are described in detail.

A. SENSOR COMPENSATION VALIDATION

We conducted an additional experiment to validate the performance of the compensation algorithm and analyzed the results of the same session dataset.

First, it is necessary to confirm that the compensated 3-axis acceleration signals have been transformed into a desired coordinate system. Therefore, we conducted an additional experiment with one subject. The subject was asked to walk 800m while wearing two sensors on his right thigh. As shown in Fig. 7(a), one sensor was worn to fit the proposed

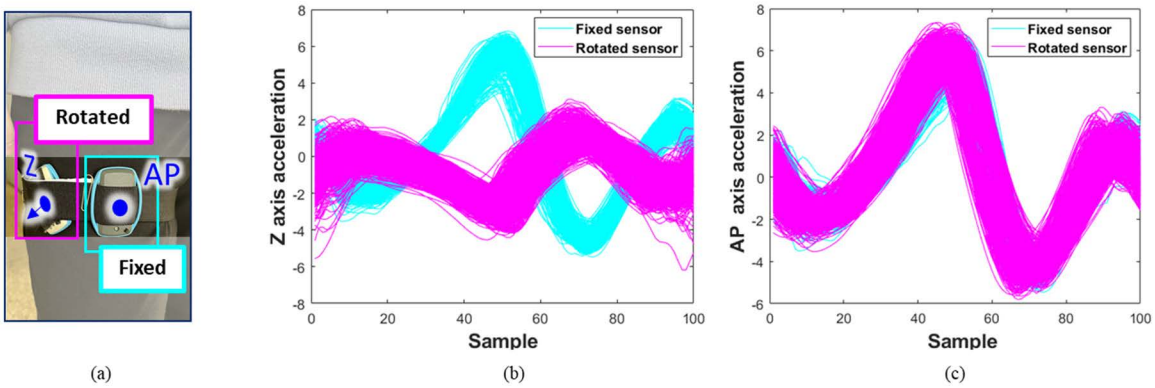

FIGURE 7. Experiments and results for compensated coordinate system verification. (a) The experimental settings, (b) z-axis acceleration cycle before compensation, (c) z-axis acceleration cycle after compensation.

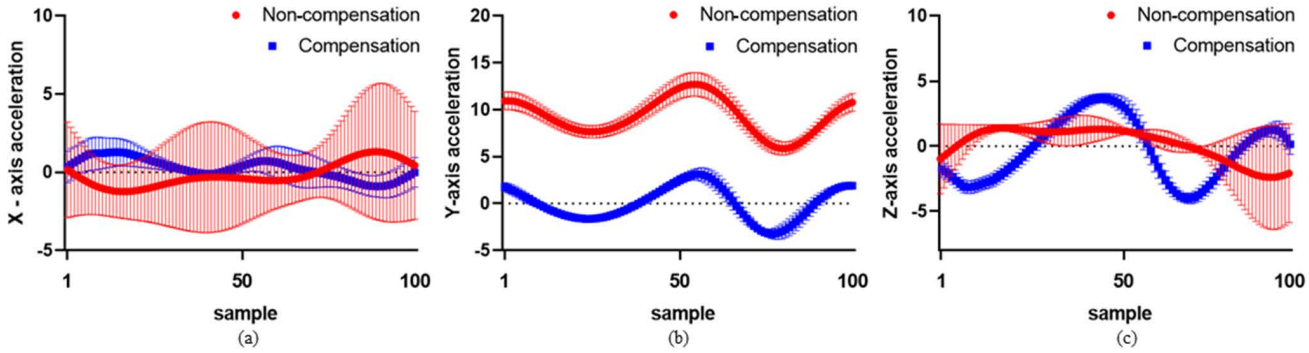

FIGURE 8. Comparison of gait cycles before and after compensation for the (a) X axis, (b) Y axis, and (c) Z axis at the thigh.

fixed-coordinate system, and the other sensor was worn while artificially creating misplacement and disorientation errors. The z-axis acceleration signals of the two sensors were not aligned with the sensor coordinate system before compensation (Fig. 7(b)), and the acceleration signals of the two sensors were aligned with the fixed-coordinate system through the compensation algorithm and converted into similar signals (Fig. 7(c)).

Next, using the validated compensation algorithm, we calculate the similarity results between the 3-axis acceleration signals from the total gait dataset of 20 participants using the cross-correlation method. Table 5 shows the similarity in acceleration signal before and after compensation in the same session. The similarity improved by 0.39, 0.01, and 0.21 at the thigh and by 0.07, 0.06, and 0.53 at the wrist in the ML, SI, and AP axes, respectively. As shown in Fig. 8, the standard deviation of all axes is significantly reduced based on the average of each sample. This suggests that the compensation algorithm transforms the data into a uniform cycle regardless of the various sensor coordinate systems.

B. USER AUTHENTICATION PERFORMANCE EVALUATION

The evaluation of user authentication is traditionally demonstrated by evaluation metrics such as Accuracy, False Acceptance Rate (FAR), False Rejection Rate (FRR), and

TABLE 5. Change of similarity before and after compensation based on cross-correlation.

	Same session data set					
	ML axis		SI axis		AP axis	
	Before	After	Before	After	Before	After
Thigh	0.58	0.97	0.95	0.96	0.74	0.95
Wrist	0.9	0.97	0.9	0.96	0.44	0.97

Equal Error Rate (EER) [41]. FAR evaluates the accepted error result in the impersonated class, and FRR evaluates the rejected error result in the user class. EER evaluates the reliability of the model as the position of the ROC (Receiver Operating Characteristic) curve when FAR and FRR are the same. Therefore, we assess the authentication performance by the average and standard error of the mean (SEM) of the evaluation metrics of individual models obtained for each person.

1) EVALUATION OF THE PROPOSED COMPENSATION ALGORITHM

We assessed the performance of the proposed compensation algorithm by comparing the Accuracy, EER, FRR in both the same and cross sessions using only 1D features at thigh. The results of the evaluation metrics suggest that the

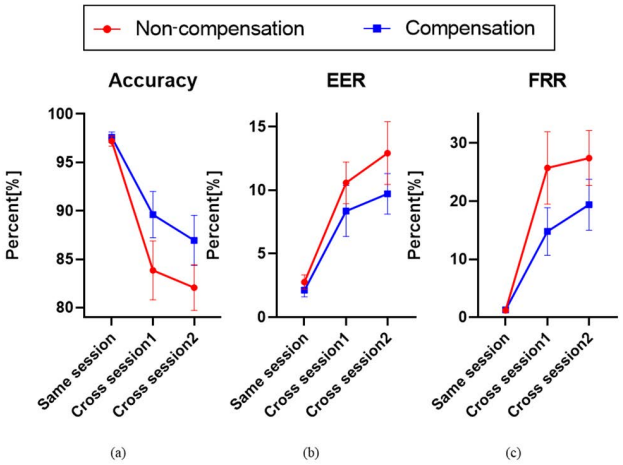

FIGURE 9. Comparison of evaluation metrics before and after compensation at the thigh (a) Accuracy, (b) EER, (c) FRR.

TABLE 6. Evaluation of proposed algorithm through comparison before and after compensation.

Metric	Sensor state	Session		
		Same session	Cross session1	Cross session2
Accuracy	Non-compensation	97.21	83.84	82.06
	Compensation	**97.60**	**89.60**	**86.94**
EER	Non-compensation	2.77	10.58	12.92
	Compensation	**2.13**	**8.36**	**9.71**
FRR	Non-compensation	1.19	25.72	27.41
	Compensation	**1.27**	**14.76**	**19.37**

EER = Equal Error Rate, FRR = False Rejection Rate

compensation algorithm outperforms the non- compensated case in all sessions, as show in Fig.9 and Table 6. The average performance of non-compensation cases degrades to less than 85% accuracy, more than 10% EER, and more than 20% FRR in the cross session scenarios. This means that the proposed compensation algorithm is robust against gait variability and external factors (e.g., different clothes, mood, health condition).

2) EVALUATION OF THE PROPOSED FEATURE EXTRACTION METHOD

We evaluated the validity of the proposed 2D feature set by comparing the EER values of the 1D general feature set and finding the optimal feature set that resulted in the best authentication performance.

The results depicted in Fig. 10 compare the performance on various sessions and positions considering various features, including general sets, cyclogram sets, and fusion sets (general + cyclogram). The 2D cyclogram feature set shows better average EER and SEM compared to the 1D feature set in all sessions and sensor positions. This means that the 2D cyclogram feature set is more distinct and unique for

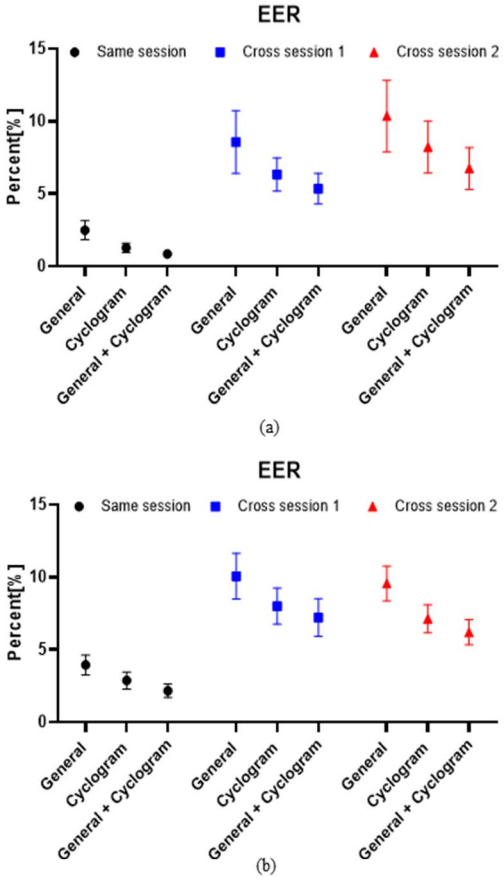

FIGURE 10. Performance comparison on feature sets by sensor position (a) at the thigh and (b) at the wrist.

representing gait characteristics and is more robust against gait variability over time. Upon validating the proposed 2D cyclogram feature set, we found it again to outperform the 1D general feature set. In addition, the performance of the fusion feature set is more effective than that of the individual feature set. This suggests that a large number of features are beneficial in cross sessions. Therefore, we analyzed user authentication performance using both feature sets.

3) PERFORMANCE EVALUATION ACCORDING TO SENSOR POSITION

We compared user authentication performance based on Accuracy, FAR, FRR, and EER metrics according to sensor position at the thigh or wrist and analyzed the results for each sensor position in detail. In addition, we assess authentication performance using both sensor positions. To integrate both feature vectors into the model, we concatenate different position feature vectors into a single feature vector. In Section III-F, we already extracted selected feature vectors of X' and Y' from each thigh and wrist. The resultant feature vector can be obtained by X' and Y'.

First, we evaluated the impact of sensor position on authentication performance for each session. The results depicted in Fig. 11 indicate that all metrics except FRR

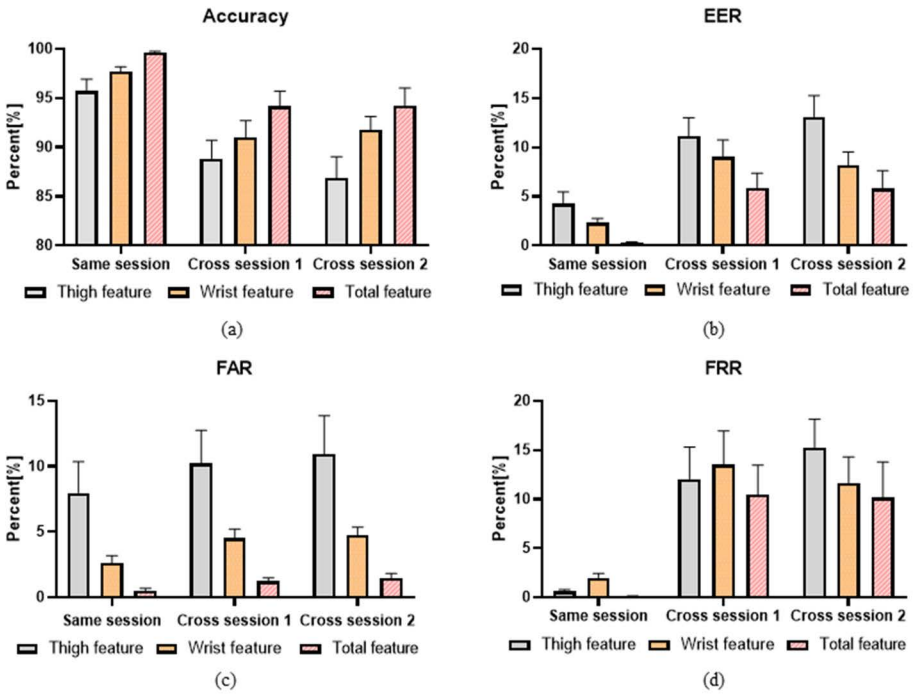

FIGURE 11. Evaluation metrics of authentication for each position and session. (a) Accuracy, (b) EER, (c) FAR, and (d) FFR.

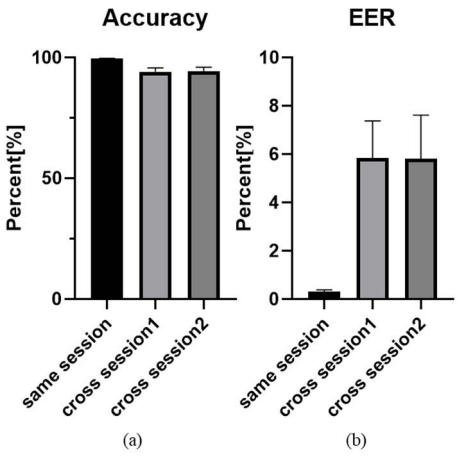

FIGURE 12. Performance of the proposed gait-based user authentication system as (a) Accuracy and (b) EER.

show better performance with the wrist than the thigh sensor. On the other hand, the FRR of the same session and cross session 1 show different tendencies. However, authentication is necessary to focus on FAR rather than FRR because prevention of personal information leakage is the priority. Also, since the results using both sensors showed better performance than measuring at each position individually, the performance of the gait cycle was analyzed using both sensor positions.

Next, we evaluated the impact of gait variability over time on authentication performance with both sensor positions. The authentication model is generated with a randomly selected training set (70%) from the same session dataset. Same session evaluation assesses the model with remaining data (30%), and the cross session evaluation assesses the model with different day data than the generated model. As shown in Fig. 12 and Table 7, the respective accuracy of cross session 1 and cross session 2 was 94.16% and 94.2%, and the EER was 5.84% and 5.8%. The performance of the proposed method is slightly worse than the same session evaluation, as the cross session evaluation tends to occur over numerous factors between training data and test data. This means that cross session evaluation is essential to clearly discuss the performance of the algorithm. All of the results show good performance, and the cross sessions show similar performance to one another. This means that stable and consistent data can be obtained despite the variability of gait over time, and that gait is a permanent biometric.

4) PERFORMANCE EVALUATION ACCORDING TO NUMBER OF GAIT CYCLES

We analyzed the impact of the number of gait cycles on authentication performance using the majority voting method [41] based on Accuracy, FAR, FRR, and EER.

As shown in Fig. 13, the authentication performance increases with the number of cycles. In particular, the performance when using all sessions showed greater than 95% accuracy and less than 5% EER, and FAR increases rapidly when using more than 3 continuous gait cycles. Based on the results of measurement time and performance,

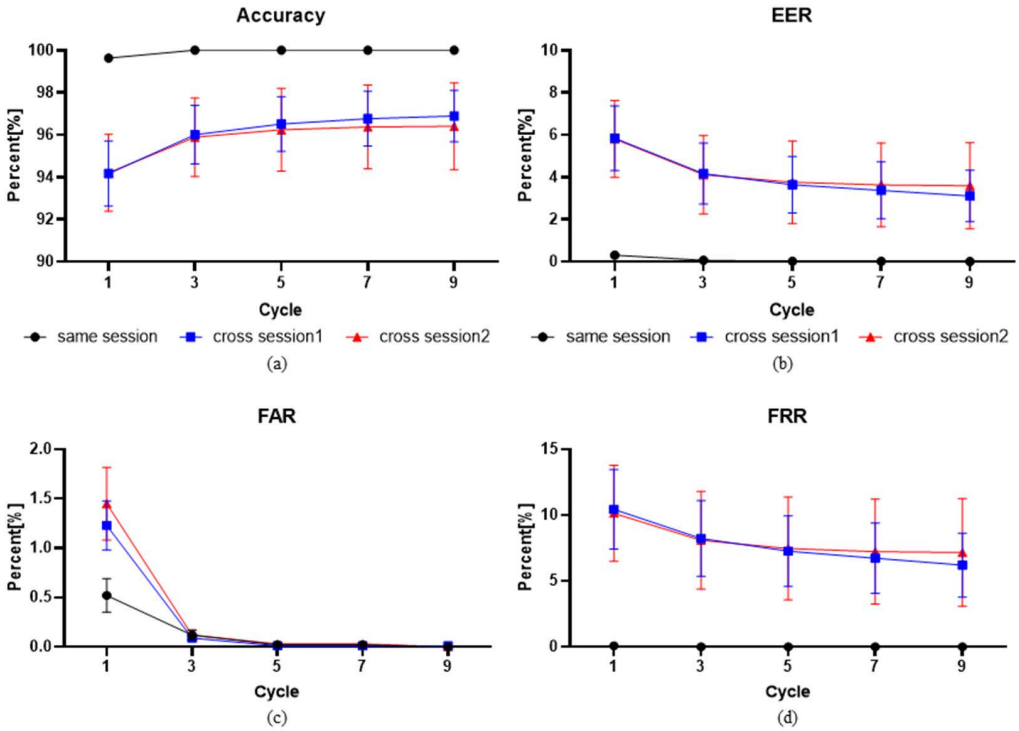

FIGURE 13. Evaluation metrics of authentication according to the number of cycles. (a) Accuracy, (b) EER, (c) FAR, and (d) FRR.

TABLE 7. The average accuracy, EER, FAR, and FRR for each position and session.

Metric	Position	Session		
		Same session	Cross session 1	Cross session 2
Accuracy	Thigh	80	88.86	86.89
	Wrist	97.7	91	91.79
	Total	**99.63**	**94.16**	**94.2**
EER	Thigh	4.27	11.14	13.11
	Wrist	2.3	9.02	8.2
	Total	**0.3**	**5.84**	**5.8**
FAR	Thigh	7.98	10.23	10.95
	Wrist	2.62	4.51	4.77
	Total	0.52	1.23	1.45
FRR	Thigh	0.57	12.06	15.28
	Wrist	1.99	13.5	11.63
	Total	0.08	10.44	10.14

FAR = False Acceptance Rate

the application of 3 continuous gait cycles is appropriate considering the performance and user-friendly.

V. DISCUSSION

Many factors can affect the performance of a gait-based user authentication system, such as sensor statement, walking speed, body condition, and user mood. As shown in Fig. 12, the performance of the proposed method decreases in cross sessions. This means that it is necessary to validate the permanence of the algorithm using data from multiple sessions and to consider various factors as well as gait information. We constructed a gait dataset that takes into account multiple days, diverse sensor positions, and statements. Our study has the advantage of performing analysis considering several factors and recommends optimized conditions for gait-based user authentication.

Most studies have used the physical fixation method to reduce the adverse effects of coordinate system variability when measuring over multiple days. For example, previous gait authentication studies use a smartwatch [19] and a waist pouch [29] that is fixed in a certain position. In this study, we solve physical fixation limitations using our proposed compensation algorithm so that it can be applied to various devices and circumstances. The compensated gait signal can be analyzed on the anatomical plane, which is a fixed coordinate system, enabling accurate behavioral analysis. This not only contributes to the improvement of authentication performance, but also allows application to movement analysis and fault diagnosis.

We propose a novel feature set that can represent an individual's unique gait characteristics. Cyclogram features contain a variant pattern for each user. In particular, the morphological curvature or distance between the center of mass and origin (0,0) has significantly different values for each individual depending on walking speed and pattern. For example, the curvature increases as walking speed increases, and components of the walking pattern are related to the distance between the center of mass and (0,0). The cyclogram

feature set that represents an individual's gait characteristics would be a better performance authentication strategy.

The results of the proposed user authentication method demonstrate average performance within the ranges of feasibility and reliability. The proposed method achieves an accuracy of 99.63%, 94.16%, and 94.20% and EER of 0.3%, 5.84%, and 5.8% in same session, cross session 1, and cross session 2, respectively. This means that the proposed method can acquire stable data despite the variability of gait over time, and that gait-based authentication can ensure the characteristics of permanence, distinctiveness, and performance. Also, as authentication performance improves with gait cycles, an increase in user effort would produce more accurate authentication performance. In particular, when 3 or more gait cycles are used, the accuracy of all sessions is greater than 95%, and the EER of all sessions is 5% or less. It is recommended to use 3 cycles in consideration of security and convenience.

VI. CONCLUSION AND FUTURE WORKS

In this study, we propose a sensor compensation algorithm that can obtain consistent gait data in any situation and extract a cyclogram feature set that can represent gait characteristics distinctly. In addition, we demonstrate the permanence of the proposed algorithm and analyze the impact on authentication performance of sensor position and number of gait cycles.

The proposed method evaluated the performance of 20 people for multiple days and various sensor positions and statements. The compensation algorithm significantly improved the similarity between the 3-axis non-compensated and compensated signals collected at both the thigh and wrist. In addition, the average EER and SEM of the cyclogram features are superior to those of the 1D general features. Authentication performance is highest when both sensors are used, although the sensor position has higher accuracy on the wrist than on the thigh. We showed that the proposed authentication method is reliable, with EERs of 0.3%, 5.84%, and 5.8% for the same session, cross session 1, and cross session 2, respectively. In addition, we concluded that using 3 gait cycles is most efficient in consideration of authentication performance and user convenience.

The gait dataset used in this study was constructed in a laboratory environment for precise analysis and evaluation of the algorithms. In future work, we will evaluate the proposed method in an uncontrolled environment. In addition, it will be necessary to apply the proposed algorithm to commercial devices to analyze various factors and develop advanced algorithms.

ACKNOWLEDGMENT

(Soobin Lee and Seungjae Lee contributed equally to this work.)

REFERENCES

[1] H. Saevanee, N. Clarke, S. Furnell, and V. Biscione, "Continuous user authentication using multi-modal biometrics," *Comput. Secur.*, vol. 53, pp. 234–246, Sep. 2015, doi: 10.1016/J.COSE.2015.06.001.

[2] M. D. Marsico and A. Mecca, "A survey on gait recognition via wearable sensors," *ACM Comput. Surv.*, vol. 52, no. 4, pp. 1–39, 2019.

[3] A. J. Aviv, K. Gibson, E. Mossop, M. Blaze, and J. M. Smith, "Smudge attacks on smartphone touch screens," in *Proc. 4th USENIX Workshop Offensive Technol.*, 2010, pp. 1–10.

[4] F. Schaub, R. Deyhle, and M. Weber, "Password entry usability and shoulder surfing susceptibility on different smartphone platforms," in *Proc. 11th Int. Conf. Mobile Ubiquitous Multimedia*, 2012, pp. 1–10.

[5] L. O'Gorman, "Comparing passwords, tokens, and biometrics for user authentication," *Proc. IEEE*, vol. 91, no. 12, pp. 2021–2040, Dec. 2003, doi: 10.1109/JPROC.2003.819605.

[6] A. Dantcheva, P. Elia, and A. Ross, "What else does your biometric data reveal? A survey on soft biometrics," *IEEE Trans. Inf. Forensics Security*, vol. 11, no. 3, pp. 441–467, Mar. 2016, doi: 10.1109/TIFS.2015.2480381.

[7] A. Jain and A. Ross, *Introduction to Biometrics*. London, U.K.: Springer, 2011, pp. 1–47.

[8] L. M. Mayron, "Biometric authentication on mobile devices," *IEEE Secur. Privacy*, vol. 13, no. 3, pp. 70–73, May 2015, doi: 10.1109/MSP.2015.67.

[9] T. Chugh, K. Cao, and A. K. Jain, "Fingerprint spoof detection using minutiae-based local patches," in *Proc. IEEE Int. Joint Conf. Biometrics (IJCB)*, Oct. 2017, pp. 581–589.

[10] J. Määttä, A. Hadid, and M. Pietikäinen, "Face spoofing detection from single images using texture and local shape analysis," *IET Biometrics*, vol. 1, no. 1, pp. 3–10, 2012, doi: 10.1049/IET-BMT.2011.0009.

[11] P. Gupta, S. Behera, M. Vatsa, and R. Singh, "On iris spoofing using print attack," in *Proc. 22nd Int. Conf. Pattern Recognit.*, Aug. 2014, pp. 1681–1686, doi: 10.1109/ICPR.2014.296.

[12] F. Miao, S. Bao, and Y. Li, "Biometric key distribution solution with energy distribution information of physiological signals for body sensor network security," *IET Inf. Secur.*, vol. 7, no. 2, pp. 87–96, Jun. 2013, doi: 10.1049/IET-IFS.2012.0104.

[13] F. Sun, C. Mao, X. Fan, and Y. Li, "Accelerometer-based speed-adaptive gait authentication method for wearable IoT devices," *IEEE Internet Things J.*, vol. 6, no. 1, pp. 820–830, Feb. 2019, doi: 10.1109/JIOT.2018.2860592.

[14] M. O. Derawi, "Smartphones and biometrics: Gait and activity recognition," Ph.D. dissertation, Dept. Comput. Sci., Gjøvik Univ., Gjøvik, Norway, 2012.

[15] S. Sprager and M. Juric, "Inertial sensor-based gait recognition: A review," *Sensors*, vol. 15, no. 9, pp. 22089–22127, Sep. 2015, doi: 10.3390/S150922089.

[16] D. Gafurov, "Performance and security analysis of gait-based user authentication," Ph.D. dissertation, Dept. Comput. Sci., Oslo Univ., Oslo, Norway, 2008.

[17] D. Gafurov, E. Snekkenes, and P. Bours, "Spoof attacks on gait authentication system," *IEEE Trans. Inf. Forensics Security*, vol. 2, no. 3, pp. 491–502, Sep. 2007, doi: 10.1109/TIFS.2007.902030.

[18] G. Cola, M. Avvenuti, F. Musso, and A. Vecchio, "Gait-based authentication using a wrist-worn device," in *Proc. 13th Int. Conf. Mobile Ubiquitous Syst., Comput., Netw. Services*, Nov. 2016, pp. 208–217, doi: 10.1145/2994374.2994393.

[19] A. H. Johnston and G. M. Weiss, "Smartwatch-based biometric gait recognition," in *Proc. IEEE 7th Int. Conf. Biometrics Theory, Appl. Syst. (BTAS)*, Sep. 2015, pp. 1–6.

[20] T. Hoang, D. Choi, and T. Nguyen, "On the instability of sensor orientation in gait verification on mobile phone," in *Proc. 12th Int. Conf. Secur. Cryptogr.*, 2015, pp. 148–159, doi: 10.5220/0005572001480159.

[21] M. Abuhamad, A. Abusnaina, D. Nyang, and D. Mohaisen, "Sensor-based continuous authentication of smartphones' users using behavioral biometrics: A contemporary survey," *IEEE Internet Things J.*, vol. 8, no. 1, pp. 65–84, Jan. 2021, doi: 10.1109/JIOT.2020.3020076.

[22] A. Al Abdulwahid, N. Clarke, I. Stengel, S. Furnell, and C. Reich, "Continuous and transparent multimodal authentication: Reviewing the state of the art," *Cluster Comput.*, vol. 19, no. 1, pp. 455–474, Mar. 2016, doi: 10.1007/S10586-015-0510-4.

[23] J. Man and B. Bhanu, "Individual recognition using gait energy image," *IEEE Trans. Pattern Anal. Mach. Intell.*, vol. 28, no. 2, pp. 316–322, Feb. 2006, doi: 10.1109/TPAMI.2006.38.

[24] L. Wang, H. Ning, T. Tan, and W. Hu, "Fusion of static and dynamic body biometrics for gait recognition," *IEEE Trans. Circuits Syst. Video Technol.*, vol. 14, no. 2, pp. 149–158, Feb. 2004, doi: 10.1109/TCSVT.2003.821972.

[25] G. D. Orr and R. J. Abowd, "The smart floor: A mechanism for natural user identification and tracking," in *Proc. CHI Conf. Hum. Factors Comput. Syst.*, 2000, pp. 275–276, doi: 10.1145/633451.633453.

[26] K. A. Sidek, V. Mai, and I. Khalil, "Data mining in mobile ECG based biometric identification," *J. Netw. Comput. Appl.*, vol. 44, pp. 83–91, Sep. 2014, doi: 10.1016/J.JNCA.2014.04.008.
[27] L. Middleton, A. A. Buss, A. Bazin, and M. S. Nixon, "A floor sensor system for gait recognition," in *Proc. 4th IEEE Workshop Autom. Identificat. Adv. Technol.*, Mar. 2005, pp. 171–176.
[28] W. Xu, G. Lan, Q. Lin, S. Khalifa, M. Hassan, N. Bergmann, and W. Hu, "KEH-gait: Using kinetic energy harvesting for gait-based user authentication systems," *IEEE Trans. Mobile Comput.*, vol. 18, no. 1, pp. 139–152, Jan. 2019, doi: 10.1109/TMC.2018.2828816.
[29] H. Alobaidi, N. Clarke, F. Li, and A. Alruban, "Real-world smartphone-based gait recognition," *Comput. Secur.*, vol. 113, Feb. 2022, Art. no. 102557, doi: 10.1016/J.COSE.2021.102557.
[30] M. Abo-Zahhad, S. M. Ahmed, and S. N. Abbas, "Biometric authentication based on PCG and ECG signals: Present status and future directions," *Signal, Image Video Process.*, vol. 8, no. 4, pp. 739–751, May 2014.
[31] Bosch Sensortec. *Sensor Fusion Software*. Accessed: 2013. [Online]. Available: https://www.bosch-sensortec.com/software-tools/software/sensor-fusion-software/
[32] M. Tschiedel, M. F. Russold, E. Kaniusas, and M. Vincze, "Real-time limb tracking in single depth images based on circle matching and line fitting," *Vis. Comput.*, vol. 38, no. 8, pp. 2635–2645, Aug. 2022, doi: 10.1007/S00371-021-02138-X.
[33] H. Zhao, L. Zhang, S. Qiu, Z. Wang, N. Yang, and J. Xu, "Pedestrian dead reckoning using pocket-worn smartphone," *IEEE Access*, vol. 7, pp. 91063–91073, 2019, doi: 10.1109/ACCESS.2019.2927053.
[34] F. Danion, E. Varraine, M. Bonnard, and J. Pailhous, "Stride variability in human gait: The effect of stride frequency and stride length," *Gait Posture*, vol. 18, no. 1, pp. 69–77, 2003.
[35] J. Benesty, J. Chen, Y. Huang, and I. Cohen, "Pearson correlation coefficient," in *Noise Reduction in Speech Processing*, vol. 2. Berlin, Germany: Springer, 2009, pp. 1–4, doi: 10.1007/978-3-642-00296-0_5.
[36] K. Tchelet, A. Stark-Inbar, and Z. Yekutieli, "Pilot study of the EncephaLog smartphone application for gait analysis," *Sensors*, vol. 19, no. 23, p. 5179, Nov. 2019, doi: 10.3390/S19235179.
[37] D. M. Henderson, "Euler angles, quaternions, and transformation matrices for space shuttle analysis," McDonnell-Douglas Tech. Services Co., Houston, TX, USA, Tech. Rep. DN-1.4-8-020, 1977.
[38] S. O. H. Madgwick, A. J. L. Harrison, and R. Vaidyanathan, "Estimation of IMU and MARG orientation using a gradient descent algorithm," in *Proc. IEEE Int. Conf. Rehabil. Robot.*, Jun. 2011, pp. 1–7.
[39] J. H. Park, H. Lee, J.-S. Cho, I. Kim, J. Lee, and S. H. Jang, "Effects of knee osteoarthritis severity on inter-joint coordination and gait variability as measured by hip-knee cyclograms," *Sci. Rep.*, vol. 11, no. 1, pp. 1–8, Dec. 2021, doi: 10.1038/S41598-020-80237-W.
[40] K. Kira and L. A. Rendell, "A practical approach to feature selection," in *Machine Learning Proceedings 1992*. San Mateo, CA, USA: Morgan Kaufmann, 1992, doi: 10.1016/B978-1-55860-247-2.50037-1.
[41] L. Lam and C. Y. Suen, "Application of majority voting to pattern recognition: An analysis of its behavior and performance," *IEEE Trans. Syst., Man, Cybern., A, Syst. Hum.*, vol. 27, no. 5, pp. 553–568, Sep. 1997, doi: 10.1109/3468.618255.

SOOBIN LEE received the B.S. degree from the Department of Medical and Mechatronics Engineering, Soonchunhyang University, South Korea, in 2021. She is currently pursuing the M.S. degree in biomedical engineering with Hanyang University, South Korea. Her current research interests include biomedical measurement systems, wearable devices, bio-signal analysis, machine learning, and user authentication based on gait.

SEUNGJAE LEE received the B.S. degree from the Department of Biomedical Engineering, Yonsei University, South Korea, in 2015, and the Ph.D. degree in biomedical engineering from Hanyang University, South Korea, in 2022. His current research interests include biomedical measurement systems, human motion analysis, and stress assessment based on heart rate variability analysis.

EUNKYOUNG PARK received the Ph.D. degree in biomedical engineering from Hanyang University, South Korea, in 2015. From 2015 to 2021, he was a Principal Research Engineer at the Biomedical Engineering Research Center, Samsung Medical Center and a Research Professor at SAIHST, Sungkyunkwan University, South Korea. He has been at Soonchunhyang University, South Korea, since 2021, where he is currently a Professor with the Department of Medical and Mechatronics Engineering. He has advanced research experience in neuromodulation, neurophysiology, and technology development. His research interests include neuromodulation and innovating medical technology for refractory disease.

JONGSHILL LEE received the B.Sc., M.Sc., and Ph.D. degrees in electronic engineering from Inha University, Incheon, South Korea, in 1995, 1997, and 2005, respectively. From 2001 to 2005, he was a Lecturer at the Department of Electronic Engineering, Korea Polytechnic University, Siheung, South Korea, where he was engaged in research on digital signal processing and digital image processing. He is currently a Research Professor with the Department of Biomedical Engineering, Hanyang University, Seoul, South Korea. His research interests include wearable devices, gait measurement and analysis, biometric authentication, the cardiovascular systems, and wearable sensors (IMUs, PPG, ECG, etc.). He is a Guest Editor and a Topical Advisory Panel Member of the journal *Sensors*.

IN YOUNG KIM received the B.S. degree from the Department of Medicine and the M.S. and Ph.D. degrees in biomedical engineering from Seoul National University, South Korea, in 1989, 1991, and 1994, respectively. He was a Principal Investigator at the Samsung Biomedical Research Institute, South Korea, from 1994 to 1997. From 1998 to 2000, he was a Senior Researcher at the Samsung Advanced Institute of Technology. Since 2000, he has been with the Department of Biomedical Engineering, Hanyang University, South Korea, as a Professor. He has published more than 350 technical articles in peer-reviewed international journals and has 48 issued patents. His current research interests include bio-signal analysis, disease diagnosis using deep learning, and non-invasive vagus nerve stimulation.